Journal of Biomolecular Structure and Dynamics

ISSN: (Print) (Online) Journal homepage: https://www.tandfonline.com/loi/tbsd20

Structural modelling and *in silico* pharmacology of β-carboline alkaloids as potent 5-HT1A receptor antagonists and reuptake inhibitors

Yusuf Oloruntoyin Ayipo, Waleed A. Alananzeh, Iqrar Ahmad, Harun Patel & Mohd Nizam Mordi

To cite this article: Yusuf Oloruntoyin Ayipo, Waleed A. Alananzeh, Iqrar Ahmad, Harun Patel & Mohd Nizam Mordi (2022): Structural modelling and *in silico* pharmacology of β-carboline alkaloids as potent 5-HT1A receptor antagonists and reuptake inhibitors, Journal of Biomolecular Structure and Dynamics, DOI: 10.1080/07391102.2022.2104376

To link to this article: https://doi.org/10.1080/07391102.2022.2104376

View supplementary material

Published online: 26 Jul 2022.

Submit your article to this journal

View related articles

View Crossmark data

Full Terms & Conditions of access and use can be found at
https://www.tandfonline.com/action/journalInformation?journalCode=tbsd20

JOURNAL OF BIOMOLECULAR STRUCTURE AND DYNAMICS
https://doi.org/10.1080/07391102.2022.2104376

Taylor & Francis
Taylor & Francis Group

Check for updates

Structural modelling and *in silico* pharmacology of β-carboline alkaloids as potent 5-HT1A receptor antagonists and reuptake inhibitors

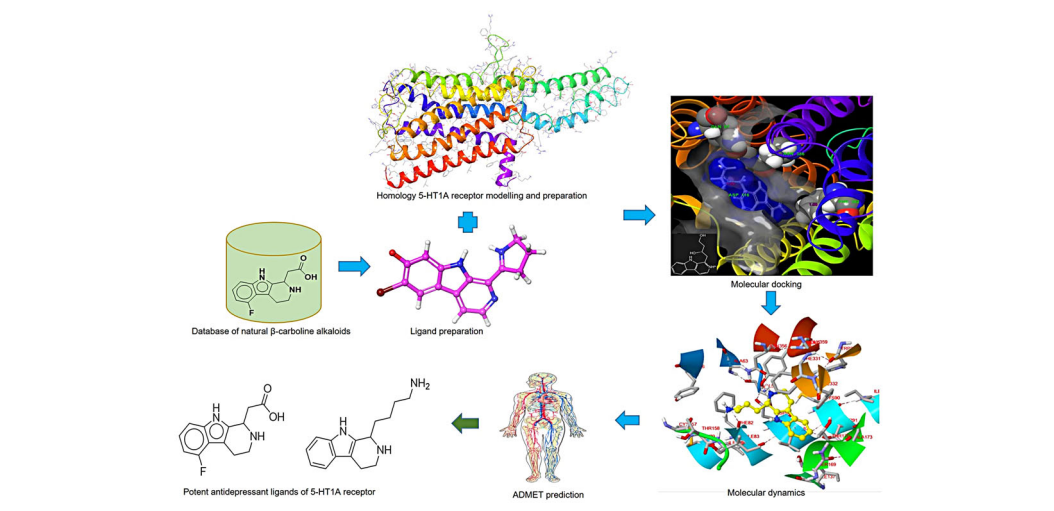
Yusuf Oloruntoyin Ayipo[a,b], Waleed A. Alananzeh[a], Iqrar Ahmad[c], Harun Patel[c] and Mohd Nizam Mordi[a]

[a]Centre for Drug Research, Universiti Sains Malaysia, USM, Pulau Pinang, Malaysia; [b]Department of Chemistry and Industrial Chemistry, Kwara State University, Malete, Ilorin, Nigeria; [c]Department of Pharmaceutical Chemistry, R. C. Patel Institute of Pharmaceutical Education and Research, Shirpur, Maharashtra, India

Communicated by Ramaswamy H. Sarma

ABSTRACT

Serotonin (5-HT) antagonists and reuptake inhibitors (SARIs) are atypical antidepressants for managing major depressive disorder. They are oftentimes applied as adjuvants for ameliorating aftereffects of SSRI antidepressants including insomnia and sexual dysfunction. The few available candidates of this class including lorpiprazole and trazodone also display some daunting side effects, making a continuous search for improved alternatives essential. Natural β-carboline alkaloids (NβCs) are interestingly renowned with broad pharmacological spectrum against several neuropsychiatric disorders including depression. However, their potentials as SARIs remain underexplored. In this study, 982 NβCs retrieved from the Ambinter-Greenpharma (Amb) database were virtually screened for potent SARI alternatives using computational and biocheminformatics approaches: homology modelling of 5-HT1A receptor, Glide HTVS, SP and XP molecular docking, molecular dynamics (MD) simulation, ADMET and mutagenicity predictions. The homology receptor was validated as a good representative of human 5HT1A receptor using the RCSB structure validation and quality protocols. From the virtual screening against the 5-HT1A receptor, Amb ligands, **Amb18709727** and **Amb37857532** showed higher binding affinities by XP scores of −8.725 and −7.976 kcal/mol, and MMGBSA of −87.972 and −107.585 kcal/mol respectively compared to **lorpiprazole,** a reference SARI with XP score and MMGBSA of −6.512 and −62.788 kcal/mol respectively. They maintained ideal contacts with pharmacologically essential amino acid residues implicated in SARI mechanisms and expressed higher stability and compactness than lorpiprazole throughout the trajectories of 100 ns MD simulation. They also displayed interesting ADME, druggability, low toxicity and mutagenicity profiles, ideal for CNS drug prospects, thus, recommended as putative SARI candidates for further study.



ARTICLE HISTORY
Received 22 April 2022
Accepted 15 July 2022

KEYWORDS
Major depressive disorder; structural modelling; molecular pharmacology; molecular dynamics; drug design

CONTACT Yusuf Oloruntoyin Ayipo yusuf.ayipo@kwasu.edu.ng Centre for Drug Research, Universiti Sains Malaysia, USM, Pulau Pinang 11800, Malaysia

Supplemental data for this article can be accessed online at http://dx.doi.org/10.1080/07391102.2022.2104376.

© 2022 Informa UK Limited, trading as Taylor & Francis Group

Abbreviations: 5-HT: serotonin; SARI: serotonin antagonist and reuptake inhibitor; NβC: natural β-carboline; HTVS: high throughput virtual screening; SP: standard precision; XP: extra precision; ADMET: absorption, distribution, metabolism, excretion and toxicity; MMGBSA: molecular mechanics generalized Born and surface area; MD: molecular dynamics; CNS: central nervous system; MDD: major depressive disorder; MAO: monoamine oxidase; SSRI: selective serotonin reuptake inhibitor; GABA: γ-aminobutyric acid; SDF: structure data file; βC: β-carboline; PDB: protein data bank; 2D: 2-dimensional; 3D: 3-dimensional; OPLS: optimized potentials for liquid simulations; RMSD: root mean square deviation; RMSF: root mean square fluctuation; SAR: structure-activity relationship; SID: simulation interaction diagram; HBA: hydrogen bond acceptor; HBD: hydrogen bond donor; TPSA: topological polar surface area; MW: molecular weight; BBB: blood brain barrier; CYP: cytochrome P450; P-gp: P-glycoprotein

Introduction

Major depressive disorder (MDD) is a debilitating psychiatric condition, characterised by irritability, generalised anxiety, insomnia, compulsive behaviour and post-traumatic stress, leading to morbidity and mortality. It seriously contributes to suicide ideation, disability-adjusted life years and the global burden of diseases (Yusuf Oloruntoyin Ayipo et al., 2021; Kochanowska-Karamyan et al., 2020). Although, the underlying pathophysiology of MDD remains yet to be fully understood, however, genetic, social, physiological and psychological factors are mainly associated with its aetiological onset development (Ferraz et al., 2019). At the cellular and molecular levels, depression is caused by low levels of monoamine neurotransmitters such as noradrenaline, dopamine and serotonin (5-HT) as well as their metabolites at the synapses, according to the monoamine hypothesis (Yusuf Oloruntoyin Ayipo et al., 2021; Yohn et al., 2017). Being ubiquitous, polygenic and multi-faceted psychiatric disorder, the effective treatment options for MDD remain challenging. The applications of tricyclic monoamine oxidase (MAO) inhibitors, selective 5-HT reuptake inhibitors (SSRIs) and selective 5-HT antagonists and reuptake inhibitors (SARIs) constitute essential management strategies (Yusuf Oloruntoyin Ayipo et al., 2021; Yohn et al., 2017). The basic mechanisms of actions of these medications include the inhibition of 5-HT transporter receptors and/or blockade of MAOs to prevent the reuptake and degradation of neurotransmitters implicated in the pathogenesis and treatment of depression including 5-HT. However, most of the currently available chemotherapeutic interventions for the pharmacological pathways in MDD conditions are challenged by delayed actions, low efficacy and unpleasant aftereffects. (Kochanowska-Karamyan et al., 2020). For instance, the medicinal application of the most commonly prescribed SSRIs including fluoxetine and escitalopram is reportedly limited by various side effects such as nausea, gastrointestinal disturbances, anxiety, insomnia and sexual dysfunction. These shortfalls oftentimes necessitate the adjuvation of SARIs with SSRIs in the management of MDD (Fasipe, 2018). Trazodone is a popular SARI adjuvant/standalone medication for managing insomnia, sexual dysfunction and some other physiological disorders induced by the SSRIs. In addition to its mechanistic antagonism/blockade and reuptake inhibition induced on the 5-HT receptor, it antagonises α1 adrenergic receptor, inhibits the 5-HT reuptake transporter and modulates cortisol suppression of the hypothalamic-pituitary-adrenal axis. These significantly enhance its efficacy against primary and secondary insomnia forms of MDD, hypothetically due to network pharmacology. By similar antagonism to the 5-HT receptors, it also suppresses the expressions of akathisia and sexual dysfunctions stimulated by the SSRIs through the 5-HT neurotransmitter. However, together with other common SARI antidepressants including lorpiprazole and lubazodone, they are also beleaguered by various degrees of side effects. These range from mild such as sedation, dizziness, dry mouth, vomiting and blurred vision to chronic ones including weight gain, orthostatic hypotension and priapism (Yusuf Oloruntoyin Ayipo et al., 2021; Fasipe, 2018; Jaffer et al., 2017; Krystal, 2013; Taciak et al., 2018).

Generally, several natural psychoactive products with psychedelic and hallucinogenic effects reportedly expressed impressive antidepressant actions upon exploration (Ferraz et al., 2019; Tang & Tang, 2019). Notably, β-carboline alkaloids are structurally diverse natural/synthetic heterocyclic compounds with a characteristic tricyclic pyrido-3,4-indole ring similar to 5-HT. They were first isolated from *Peganum harmala* and subsequently from dozens of other natural sources including *Arenaria kansuensis*, *Psilocybe* mushrooms, *Acanthostrongylophora ingens*, *Annona foetida*, and *Eudistoma* spp (Blei et al., 2019; Cui et al., 2017; Ibrahim & Mohamed, 2017). Interestingly, due to their ability to interact with various biological targets, the unique class of organic compounds have been reported with a broad spectrum of pharmacological actions against several ailments including inflammation, cancer, neuropsychiatric disorders and recently coronavirus disease (Yusuf Oloruntoyin Ayipo et al., 2021; Yusuf Oloruntoyin Ayipo et al., 2021; Dai et al., 2018). In addition, βC alkaloids have been evaluated with interesting potency along the pharmacological pathways implicated in the development and effective management of MDD. These include the induction of neurogenesis and neuroendocrine response, modulation of the 5-HT, γ-aminobutyric acid (GABA) and glutamate receptors, and restoration of astrocytic functions (Ferraz et al., 2019). They are also understood to enhance serotonin (5-HT) levels in the tissues through reversible competitive inhibition of the monoamine oxidases A and B, effective binding to the 5-HT receptors, the immunoregulators in both vertebrates and invertebrates. The pharmacological implications of the interactions include an increase in the levels of 5-HT metabolite, 5-hydroxy indole acetic acid (5-HIAA) and homovanillic acid, a catecholamine metabolite (Wrońska & Boguś, 2019).

Despite the interesting neuropharmacology, the evaluation of vast NβC alkaloids as improved and safer candidates for SARIs remain underexplored. Moreover, the application of computer-aided drug design has been supporting a faster, cheaper and environmentally friendly approach towards screening a large molecular database and identify the most promising candidates for specific ailments. The scientific approach has successfully enhanced the discovery of drug alternatives with top-notch medicinal values worthy of replacing the existing ones (Phillips et al., 2018).

Thus, this study is aimed at the evaluation of NβC alkaloids from the Ambinter-Greenpharma chemical library (https://www.ambinter.com/) as potent SARIs using a computational and molecular modelling approach. The human 5-HT1A receptor was modelled using server-based SWISS-MODEL (Waterhouse et al., 2018), Maestro Glide high throughput virtual screening (HTVS), standard precision (SP) and extra precision (XP) Maestro 12.12 (Schrodinger, LCC, New York, NY, 2019) docking modules were employed to investigate the interactive potentials of the NβC alkaloids as antagonists and reuptake inhibitors of 5-HT1A homology receptor. The stability of four selected ligands from the virtual screening was studied using Desmond 2020-3 (Maestro-Desmond Interoperability Tools, Schrödinger, New York, NY, 2021) molecular dynamics (MD) simulation. The physicochemical, pharmacokinetics and pharmacodynamics, as well as toxicological profiles of the selected NβCs, were predicted using Swiss ADMET (Daina et al., 2017), while VEGA ToxRead java-based software was used to study their mutagenicity *in silico* (Gini et al., 2014).

Materials and methods

Ligand selection and preparation

The Ambinter-Greenpharma chemical library of natural products (https://www.ambinter.com/) was searched for substructures of βC alkaloids. The retrieved (982) ligands were downloaded in structure data file (SDF) format for preparation. The SDF files of the retrieved βC ligands as well those of lorpiprazole, trazodone, metformin and albendazole (2 positive and 2 negative controls) were imported as 2 D structures into the workspace of Maestro 12.12 (LigPrep, Schrodinger, LCC, New York, NY, 2019). Their preparation was carried out through the protonation, energy minimization and the estimation of geometry and partial atomic charges using OPLS-3e force field (Harder et al., 2016). The default Epik at a target was maintained as pH 7.0 ± 2.0 to generate possible ionization states and the ready-to-dock minimized conformers were saved in LigPrep.out file.

Homology modelling and validation

The unavailability of a resolved crystal structure of human 5-HT1A receptor at the protein data banks (PDBs) as at the time of conducting the research necessitate homology receptor modelling. The human 5-HT1A receptor has been modelled in our previous study (Ayipo et al., 2022) using the SWISS-MODEL server (https://swissmodel.expasy.org/) (Waterhouse et al., 2018) by the input of the FASTA file of human 5-HT receptor 1 A (P08908) protein sequence retrieved from UniProtKB (https://www.uniprot.org/). A crystal structure for 5-HT1B (PDB 4IAR) was returned with highest similarity (42%) from the blast, as such, was then adopted as a template receptor. The modelled structure has been validated using RCSB structure validation and quality protocols including MolProbity (Williams et al., 2018), ProSA-web (Wiederstein & Sippl, 2007), ERRAT (Colovos & Yeates, 1993), PROVE (Pontius et al., 1996), Verify-3D (Luthy et al., 1992), NQ-Flipper (Weichenberger & Sippl, 2007) and WHATCHECK (Hooft et al., 1996) for a reliable adoption for further study (Ayipo et al., 2022). However, a crystal structure of 5-HT1A titled "Aripiprazole-bound serotonin 1 A (5-HT1A) receptor-Gi protein complex" (PDB 7E2Z) with a sequence similarity of >95% to the modelled 5-HT1A has been released to the RCSB PDB after the completion of this study. In order to revalidate the modelled receptor with the new crystal structure, comparative analyses were carried out between the two structures. Among the various chains of the complex crystal structure (PDB 7E2Z), aripiprazole, an antipsychotic drug and inhibitor of 5-HT1A receptor was co-crystallized within the active site on chain D/R (Xu et al., 2021). To find a scientific correlation between our modelled 5-HT1A receptor, AlphaFold human 5-HT1A model (https://alphafold.ebi.ac.uk/search/text/5HT1A_HUMAN?suggested=true) (Varadi et al., 2022) and the newly released crystal structure of 5-HT1A, we aligned the three structures using Maestro 12.2 (Schrodinger, LCC, New York, NY, 2019).

Protein preparation, binding site analysis and generation of the receptor grid box

The PDB format of the homology 5-HT1A receptor model was preprocessed by assigning bond order, protonation states and filling missing loops using Protein preparation wizard (Madhavi Sastry et al., 2013). Further preparation includes optimization, refining and energy minimization for the conversion of heavy atoms to relative mean standard deviation (RMSD) of 0.3Å using OPLS-3e force field of Maestro 12.12 (Harder et al., 2016). Since the homology receptor contains no co-crystallized ligand for active site detection, the receptor binding pocket was generated using a Biologics sitemap (T. Halgren, 2009). The best druggable binding site was selected based on Site score and Dscore while the grid box was assigned with x, y and z coordinates using default settings of the selected sitemap focal points and the identified amino acid residues (Marondedze et al., 2020). The active site generated by the Biologics sitemap detection was compared with the binding pocket occupied by aripiprazole in the newly released crystal structure (PDB 7E2Z) for accuracy. The ready-to-dock grid box was saved in the gridbox.zip file.

Virtual screening by molecular docking

Molecular ligand-receptor docking analysis was used to virtually investigate the inhibitory and antagonistic interactions of

the βC conformers generated from the LigPrep module against the homology 5-HT1A receptor. Both the receptor grid zip and ligand output files were uploaded for complete virtual screening through the step-wise HTVS, SP and XP molecular docking modules of Maestro 12.2 Glide (T. A. Halgren et al., 2004). The molecules were ranked in descending algorithms of the docking scores which were used for screening at each docking module. The hydrophilic and hydrophobic interactions of the selected ligands with pharmacologically essential amino acid residues in the active binding pocket of the receptor were analysed using the binding poses from the XP module. Four βCs with good scoring functions and binding interactions were selected for further studies. In addition to the validation using known positive and negative inhibitors, the docking protocols were revalidated taking the advantage of the newly published crystal structure (PDB 7E2Z) with co-crystallized 5-HT1A inhibitor, aripiprazole. The co-crystallized ligand was used to set the binding pocket of the minimized crystal structure. The co-crystallized ligand was re-docked into the active pocket of the crystal structure and the complex was superimposed with the original crystal structure for RMSD calculation. An RMSD value of $\leq$2.0 Å (the smaller the better) validates the docking protocols as accurate and precise (Castro-Alvarez et al., 2017; Ramírez & Caballero, 2018). To further validate the modelled 5-HT1A receptor with the newly released crystal structure using molecular docking, the two final hit ligands, **Amb18709727** and **Amb37857532** were redocked on the crystal structure. The docking scores and poses of the two final hits ligands were compared when docked separately on to the crystal structure and the modelled 5-HT1A receptor herein reported.

Molecular dynamics simulations

The MD simulations were performed for the homology 5-HT1A receptor as well as its complexes with the four selected βCs including the reference drug, using the academic version of Desmond 2020-3 (Maestro-Desmond Interoperability Tools, Schrödinger, New York, NY, 2021). The solvated system was built using a pre-defined TIP3P water model in the System Builder panel. The ligand-receptor complex for each βC as well as the referenced lorpiprazole was centred in an orthorhombic cubic box with periodic boundary filled with Single-point charge (SPC) water molecules buffered at a minimum distance of 10 Å units between a protein atom and box edges. The charges of the complex systems were electrically neutralised with an adequate number of counter-ions (Na^+ and Cl^-), and an isosmotic state was maintained by adding 0.15 M NaCl. The energies of the complexes were minimized by heating and equilibrium processes and relaxed using the OPLS 2005 force field with other parameters of Desmond at default (Iqrar Ahmad et al., 2021; Jorgensen et al., 1996; Mohankumar et al., 2020; Patel et al., 2021). The MD simulations were carried out using a Nose-Hoover method with an isothermal-isobaric/NPT ensemble with 300 K temperature, 1 atm pressure, and a 200 ps thermostat relaxation period (Mohankumar et al., 2020; Nosé, 1984). The systems were normalised in equilibrium states with a total number of 1000 trajectories produced within the 100 ns period. The results were analysed using the Simulation Interaction Diagram (SID) tool and the best ligand-receptor conformations were selected based on their interactions and dynamic properties for stability and flexibility (I. Ahmad et al., 2021; Mohankumar et al., 2020). The average fluctuation in the displacement of a selection of atoms for a certain frame concerning a reference frame is observed by the RMSD plot, considering the Cα atoms for calculations while the RMSF plot reveals the characteristic local fluctuations along the protein chain (Patel et al., 2021). Equations (i) and (ii) (D. E. Shaw Research, 2021; Zrieq et al., 2021) were computationally applied to estimate the RMSD and RMSF.

$$RMSD_x = \sqrt{\frac{1}{N}\sum_{i=1}^{N}\left(r_i'(t_x)\right) - r_i(t_{ref}))^2} \quad \text{(i)}$$

$$RMSF_i = \sqrt{\frac{1}{T}\sum_{t=1}^{T} < \left(r_i'(t)\right) - r_i(t_{ref}))^2 >} \quad \text{(ii)}$$

Calculation of binding free energy by MMGBSA method

The post-simulation molecular mechanics generalised Born and surface area (MM/GBSA) analysis was conducted partly to support the validity of the inhibitory mechanisms of the ligands against the receptor in the absence of experimental validation. Both MM/PBSA and MM/GBSA have been regarded as efficient computational methods for binding free energy calculations, and they have been successfully applied in many aspects of drug design, including structure-based virtual screening, lead optimization, and molecular recognition. With MMGBSA, protein–ligand and protein–protein interaction energies can be relatively estimated more quickly and accurately as an absolute sum of gas-phase, entropy contributions and solvation free energy over snapshots from MD trajectory when compared with alchemical free energy methods. Moreover, the method is reportedly less sensitive to calculation disparity arising from the application of different force fields, implicating a good compatibility with various force fields (Forouzesh & Mishra, 2021; Sun et al., 2018). The MM/GB(SA) continuum solvation re-scoring method was applied to estimate the binding free energy of each ligand in complex with 5-HT1A receptor. The scoring function utilised includes the OPLS3 force field and VSGB solvation model. Every 100th frame was collected from the last 50 ns of simulated trajectories of each MD trajectory, averaging more than 6 frames, for lead compounds binding free energy calculations. The prime MMGBSA was simulated using the Glide pose viewer files, representing the inputs for energy minimization for each ligand-receptor complex ($G_{complex}$), the free ligand (G_{ligand}) and the free receptor ($G_{receptor}$) The MM/GB(SA) was calculated as ΔG_{bind} in the equation (iii) (Genheden & Ryde, 2015) below:

$$\Delta G_{bind} = G_{complex} - G_{receptor} - G_{ligand} \quad \text{(iii)}$$

The relative affinity of each selected ligand to the receptor is estimated using this algorithm, while a more negative value indicates a stronger binding affinity (Iqrar Ahmad et al., 2021; Genheden & Ryde, 2015).

Prediction of pharmacokinetics, pharmacodynamics and druggability

Some physicochemical, pharmacokinetics and pharmacodynamics parameters crucial to drug-like candidates were estimated for the four selected NβCs using readout of the BOILED-Egg SwissADME model by the input of SMILE strings of the molecules (http://www.swissadme.ch/) (Daina et al., 2017). The parameters including molecular weight (MW), lipophilicity (XLog P3), solubility (ESOL Log S), number of hydrogen bond acceptor/donor (HBA and HBD), flexibility (number of rotatable bonds) and topological polar surface area (TPSA) were quantitatively predicted to profile their absorption, distribution. metabolism and excretion (ADME). The druggability of the selected NβCs was also determined using the potentials for blood-brain barrier (BBB), p-glycoprotein (pg) substrate and human gastrointestinal absorption. The parameters for the selected ligands were compared with the standard drug about the Lipinski's and BDDC rules of 5 (RO5) and druggability (Benet et al., 2016; Lipinski, 2004).

In silico toxicology and mutagenicity

The toxicological and mutagenicity profiles of the selected NβCs were determined *in silico* through the potentials for interaction with superfamily cytochrome P450 (CYP) isoenzymes and modelled read-across structure-activity relationship (SAR) using Swiss ADME server and Java-based VEGA ToxRead 0.2Beta software respectively. In both cases, the string SMILE formats of the selected molecules were input into their workspace and run under default settings (Ayipo et al., 2022; Gini et al., 2014).

Final hits

The NβCs alkaloids with promising potentials as SARIs, good pharmacokinetics and pharmacodynamics profiles, and low expressions for systemic toxicity and mutagenicity were selected as final hits for further experimental and transformational studies into SARI therapeutics.

Results and discussion

Ligand selection and preparation

Exactly 982 NβC alkaloids were identified from the Ambinter-Greenpharma chemical library search and downloaded in SDF format. The ligand preparation step generated 5006 ready-to-dock minimized protonated conformers.

Revalidation of homology 5-HT1A receptor model

The homology 5-HT1A model was validated in our previous studies as good as shown in Table 1 (Ayipo et al., 2022). Since a crystal structure has been released before this submission, the modelled receptor was revalidated for similarity according to Schrodinger protocols for structure alignment. The structures of the modelled 5-HT1A receptor, the AlphaFold 5-HT1A model and new crystal structure of 5-HT1A (PDB 7E2Z) chain R were strongly aligned with an alignment score of 0.1635 and RMSD of 2.0055 Å, whereas, an alignment score between 0.0-7.0 (the smaller the better) and RMSD of 0.0-3.0 Å indicates a significant alignment with sufficient similarity. The structures of the modelled receptor and crystal structure template were well superimposed with one of the final ligand, Amb18709727 occupying their common active binding site (Figure 1 and Supplementary Figure S1) (http://gohom.win/ManualHom/Schrodinger/Schrodinger_2015-2_docs/maestro/help_Maestro/tools_menu/protein_structure_alignment.html).

The only slight difference was observed in the head and tail of the AlphaFold model sequence which extended by 34 amino acid residues (residue number 31-64) and 7 amino acid residues (residue numbers 446-452), whereas, our model only has 3 amino acid residue extensions at each end compared to the crystal structure. Moreover, the regions of slight extensions are irrelevant to the binding pockets of the receptors. In addition, the amino acid residue numbered 95 is leucine (L) in both AlphaFold and our model, whereas, it represents tryptophan (W) in the crystal structure. These insignificant differences are indicated with red squares in the supplementary Figure S1. Apart from these, the three structures, our model, AlphaFold model and crystal structure (PDB 7E2Z, chain R) have perfectly aligned sequences across local and global regions, supporting the validity of our model as a good representative of the human 5-HT1A receptor.

The homology structure obtained represents a typical phylogenic G-protein coupled receptor (GPCR) with transmembrane helices for signal processing across cell membrane and ability to transform its conformation during biological actions (Figure 2A). For a reliable adoption of the modelled receptor, the quality of the structure was validated by the RCSB-established protocols. From the validation results (Table 1, Supplementary file, Figures S2–S4), the homology 5-HT1A model attained a ranking percentile of 97, about 361 out of 386 (93.52%), residues in favoured regions, >99% residues in allowed regions and an insignificant 0.3% of residues within the disallowed region. It has a good Z-score of −5.21 and a Verify 3 D score of 57.22, a value higher than that of the receptor template (PDB 4IAR). The model was therefore validated as a good representative of the human 5-HT1A receptor in a strong similarity to the template receptor (Ayipo et al., 2022; Karim et al., 2018; Negi et al., 2019; Weichenberger et al., 2008). Moreover, the new crystal structure of 5-HT1A (PDB 7E2Z) was later included in the validation sets. Interestingly, the validation scores recorded for the new crystal structure were similar to those of the initial validation template (PDB 4IAR), and both were within the range of the results for the modelled 5-HT1AR. These further support

Table 1. Homology 5-HT1A receptor validation results in comparison with the templates PDBs 4IAR and 7E2Z.

Validators	Parameter	PDB 4IAR	PDB 7E2Z	5-HT1A model
MolProbity	Clash score	4.21	1.73	3.28
	Percentile	100	100	97
	MolProbity score	1.96	0.96	1.95
Ramachandran	Favoured region (%)	93.7	94.6	93.5
Plot	Allowed region (%)	100	100	99
	Disallowed region	0	0	0.3
ProSA-web	Model Z-core	−4.52	−4.87	−5.21
ERRAT	Quality factor	96.64	89.43	91.73
PROVE	Buried outlier protein	55 (4.1%)	7.0	58 (5%)
Verify 3 D	3D-1D> =0.2 (%)	39.05	73.91	57.22
NQ-Flipper	Erroneous Asp and Glu rotamers	0	0	0
WHAT-CHECK	No of Error Residue	4	4	5
SAVE	Overall summary	Pass	Pass	Pass

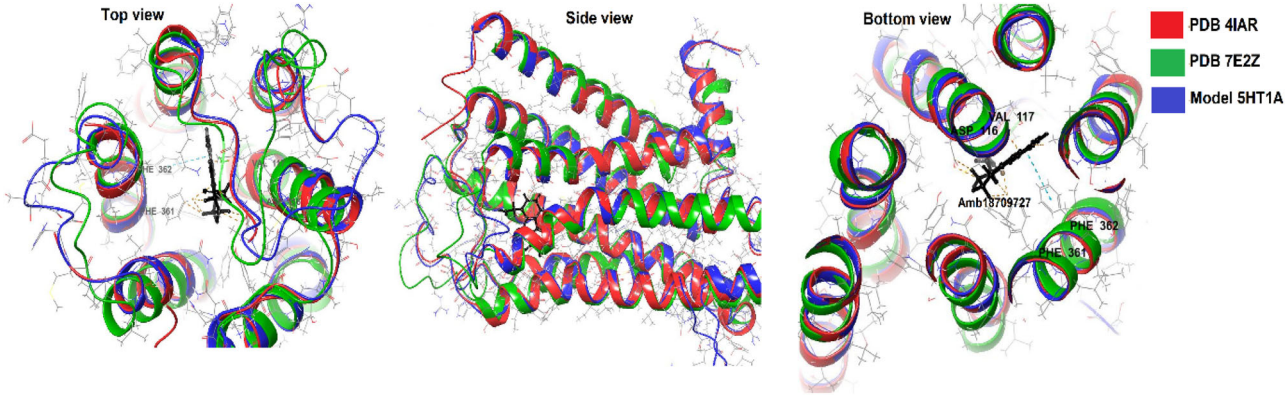


Figure 1. Superimposition of modelled 5-HT1A receptor and crystal structures of the templates (PDBs 4IAR and 7E2Z). The model receptor aligned well with the template crystal structures along the various helices and loops, indicating a good resemblance.

the validity of the modelled 5-HT1AR as a good representative receptor for the target. Thus, the modelled structure has been reliably and qualitatively adopted for further study.

Protein preparation, binding site analysis and generation of the receptor grid box

The protein preparation protocols as described in the experimental section generated a minimised structure of the model receptor. From the binding pocket analysis for the detection of the most probable druggable sites of the receptor, the Sitemap algorithms generated 5 sites ranked according to their site score and Dscore. The sites were labelled 1, 2, 3, 4 and 5 (Figure 2A) with site score of 1.098, 1.064, 0.962, 0.869 and 0.722, and Dscore of 1.138, 0.958, 1.045, 0.796 and 0.634 respectively. Site 1 has the highest site score and Dscore, thus, ideally selected as the most potent binding pocket of 5-HT1A receptor, consistently with relevant previous studies (Marondedze et al., 2020; K. Ostrowska et al., 2017; Prandi et al., 2012). Site 1 contains Asp 116, Ser 119, Phe 361, Phe 362 and Asn 386 (Figure 2A) which importantly constitute the active binding pocket of the human 5-HT1A receptor, according to some previous relevant studies, (Negi et al., 2019; K. Ostrowska et al., 2017; Ostrowska et al., 2018), thus adopted for molecular docking. The parameters of the selected site including the mapped amino acid residues were used to generate a docking grid box with x, y and z coordinates of −12.89, −15.72 and 14.06 Å respectively within a cavity volume of $30 \times 30 \times 30$ Å, saved as .zip file. Interestingly, the active site prediction here corresponds to the site occupied by aripiprazole, a 5-HT1A inhibitor co-crystallized in the newly released 5-HT1A crystal structure complex (PDB 7E2Z) (Xu et al., 2021).

The inhibitory and antagonistic interactions of the ligands were demonstrated against homology receptor at various modules of HTVS, SP and XP molecular docking. The ligands were docked deeply in the main active pocket of the G-coupled protein receptor in similarity to a renowned SARI, lorpiprazole (Figure 2B). Similarly, they occupy almost the entire volume of the main active pocket cavity of the receptor in the same manner as lorpiprazole (Figure 2C). These analogic observations hypothetically support similar mechanisms of actions between the selected ligands and lorpiprazole against 5-HT1A and support the ligands as potential SARIs for further study.

Virtual screening

The prepared ligands docked within the configured active pocket of the receptor were ranked in ascending order of docking and XP Gscores, representing their theoretical binding affinity (Table 2). The higher the negative value the higher the scores. Sixteen (16) ligands with good docking scores compared with the controls were screened after docking, constituting 1.62% of the total initial dataset. Out of the 16 ligands, four (0.4%) with higher docking scores than the controls and relevant binding poses were selected for further analysis. All the four selected NβC ligands possess higher

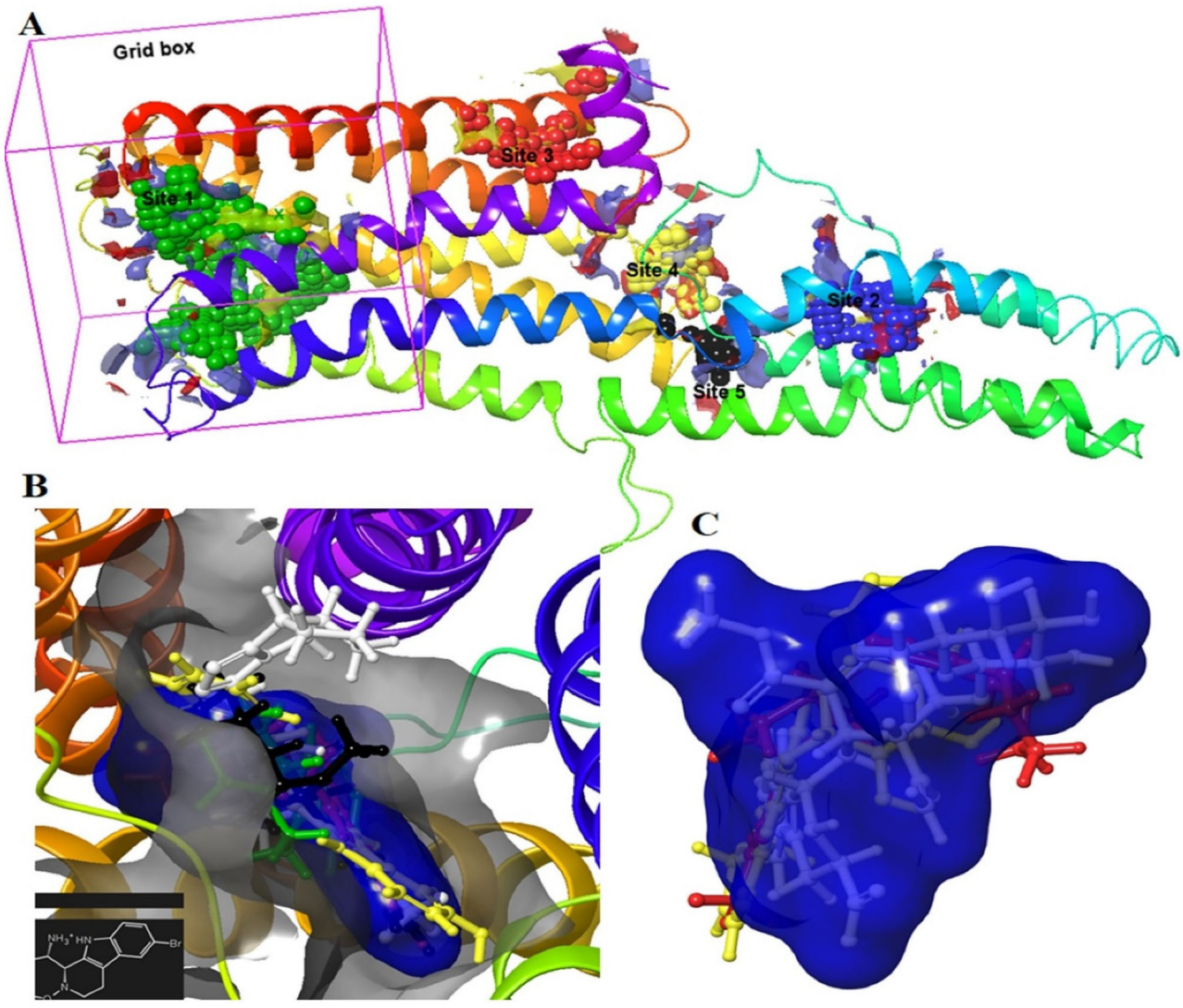


Figure 2. Receptor binding site analysis using 3 D models. (A) Druggable binding sitemaps of 5-HT1A receptor, Site 1 (green balls region) with grid box generated for docking; Site 2 (blue balls); Site 3 (red balls); Site 4 (yellow balls); Site 5 (black balls). (B) The surface of the GPCR (5-HT1A homology receptor) active pocket with selected docked NβCs in ball and stick models: ligand **Amb932777** (red), **Amb37857532** (black), **Amb35813946** (yellow), **Amb18709727** (green) and **Lorpiprazole** (white). (C) Selected NβC ligands occupy a similar volume of the open ligand binding sub-cavity of the GPCR with the reference drug, lorpiprazole.

scores than the positive antidepressant controls, lorpiprazole and trazodone, indicating higher binding affinity. The best docked NβC has XP GScore of −10.145 kcal/mol compared to the best docked positive and negative control drugs, lorpiprazole and albendazole whose scores are −6.512 and −3.835 kcal/mol respectively. Generally, the negative controls, albendazole and metformin scored least, demonstrating low binding interaction as expected, thereby supportively validated the protocols in the absence of a co-crystallized ligand.

The docking procedure was also validated as good and reproducible by the Glide RMSD value of 1.97 Å when the co-crystallized aripiprazole was redocked and superimposed onto the active site of PDB 7E2Z (Figure 3A) (Castro-Alvarez et al., 2017; Ramírez & Caballero, 2018). The active pocket amino acid residues of the crystal structure (PDB 7E2Z) where aripiprazole is bound is similar to the active pocket of our modelled 5-HT1A receptor (Figure 3B). The SP docking scores deduced for both **Amb18709727** and **Amb37857532** in complex with the crystal structure are −6.690 and −7.728 kcal/mol respectively. These are consistent with the SP docking scores of −6.994 and −7.328 kcal/mol obtained for the respective ligands against the modelled receptor (Table 2). As shown in Figure 3B, both hit ligands interacted with the amino acids residues in the active pocket of the two structures through similar bonding and non-bonding interactions, supporting the accuracy of both homology modelling, active pocket prediction and docking results. For instance, with the crystal structure (PDB 7E2Z), **Amb18709727** formed an H-bond and a salt bridge interaction with Asp 116 through NH_2, and a hydrophobic π-π interaction with Phe 362 through its benzene group. Similar interactions could be observed with the 5-HT1A model receptor with an addition of a H-bond to Ile 189 and other non-bonding van der Waals interactions. Consistently, **Amb37857532** also interacted with almost the same set of amino acid residues in both crystal structure and the 5-HT1A model through similar bonding and non-bonding interactions.

According to some relevant previous studies (Negi et al., 2019; K. Ostrowska et al., 2017; Ostrowska et al., 2018), Asp 116, Phe 361, Phe 362 and Asn 386 constitute essential residues at the active site of 5-HT1A for pharmacological

Table 2. Docking results of selected NβC ligands and reference drugs against 5-HT1A receptor.

Title	Docking Scores (kcal/mol)			Interacted amino acid residues	MMGBSA (ΔG_{Bind}) (kcal/mol)
	HTVS	SP	XP		
Amb35813946	−7.482	−8.592	−10.145	Asn 100, Ile 189, Phe 362	−46.676
Amb18709727	−6.005	−6.994	−8.725	Asp 116, Ile 189, Phe 362	−87.972
Amb37857532	−7.553	−7.328	−7.976	Asp 116, Phe 361, Phe 362, Asn 386	−107.585
Amb932777	−6.234	−6.681	−7.820	Asp 116, Ile 189, Phe 362	−51.322
Lorpiprazole	−3.680	−6.273	−6.512	Asp 116, Phe 361	−62.788
Trazodone	−3.899	−6.108	−6.835	Gln 97, Asp 116, Phe 361, Phe 362	–
Albendazole	−5.061	−4.134	−3.835	Asp 116, Phe 361	–
Metformin	−1.656	−2.551	−1.601	Gln 97, Asp 116	–

See Supplementary File 1, Table S1 for more details.

interactions. From the 2 D and 3 D binding poses (Figure 4), **lorpiprazole**, a commonly prescribed SARI antidepressant interacted with the hydrophilic amino acid, Asp 116 through H-bonding and a salt bridge to its basic NH moiety. Three βC ligands, **Amb18709727, Amb37857532** and **Amb932777** also displayed strong hydrophilic interactions with this backbone amino acid residue, Asp 116, through H-bonding and/or salt bridge formation to their basic NH groups in β-position to the indole NH. The reference inhibitor displayed hydrophobic interactions to either Phe 361, Phe 362 or both through aromatic π – π interactions. Consistently, the four selected NβCs also showed these interactions through their pharmacophoric aromatic π-system towards the same conserved helices as observed with the reference drugs, indicating identical behaviour against the receptor. The interactive phenomena support a propensity for similar inhibitory mechanisms between the selected NβCs and the known inhibitors and are determinants for the stabilization of the ligands in the active pocket of the 5-HT1A receptor (K. Ostrowska et al., 2017; Ostrowska et al., 2018; Prandi et al., 2012). The hydrophobic interactions of these NβC ligands could induce a decrease in the surface area and undesired hydrophilic participations, thereby, contributing to the folding, stability and biological activity of the 5-HT1A receptor which was reportedly hypothesised as a rigid model with Gasteiger partial charges (Dyson et al., 2006; Ostrowska et al., 2018). The interactions are similar to those displayed by aripiprazole, a 5-HT1A inhibitor co-crystallized in the newly released 5-HT1A crystal structure (PDB 7E2Z) (Xu et al., 2021). Interestingly, the selected ligands also interacted with more reserved amino acid residues in the active pocket of the receptor. For instance, ligands **Amb37857532** additionally showed H-bonding to the side chain residue, Asn 386 through NH, while **Amb35813946**, **Amb18709727** and **Amb932777** also expressed more hydrophilic interactions through Ile 189 compared to the reference drugs. Undoubtedly, these contribute to their higher binding affinity and inhibitory potentials than the reference antidepressants as observed in the docking XP scores. In addition to the bonding interactions, the non-bonding van der Waals association between the ligands and the amino acid residues also enhance the inhibitory potentials as indicated by the scoring functions.

Molecular dynamics

The structural conformation and thermodynamic stability of the protein receptor as well as its complexes with bound ligands were observed using the RMSD plot (Figure 5). The plot indicates the equilibration and fluctuations of the simulation systems throughout the trajectories. A conformational change and structural fluctuation within 1-3 Å indicate acceptable stability for small and globular proteins. It could be observed that the Apo protein became equilibrated just around 2 ns after the commencement of the simulation and remain stable thereon, experiencing an insignificant perturbation of <1 Å till the end of 100 ns simulation. Similarly, the RMSD of the heavy atoms of the selected ligands mostly became equilibrated around 0-2 ns and maintained good stabilities throughout the trajectories of simulations. From then, ligands **Amb35813946** and **Amb18709727** experienced the highest stability in complex with the protein and maintained a strong contact throughout simulation with average fluctuations of <1 Å. Although ligands **Amb37857532** and **Amb932777** showed slightly higher fluctuations, however, they were all within the acceptable $1-3$ Å for stability, without diffusing away from the binding pocket, consistently with the reference drug, **lorpiprazole**.

The RMSF plot (Figure 6) indicates the protein residues that fluctuate most along the trajectories of the simulations. The amino acid residues, Asp 116, Phe 361, Phe 362 and Asn 386 are most important for the inhibition of the 5-HT1A receptor for pharmacological expression according to relevant literature receptor (Negi et al., 2019; K. Ostrowska et al., 2017; Ostrowska et al., 2018; Prandi et al., 2012). Interestingly, these residues maintained good stabilities mostly >3 Å throughout the simulation of the Apo protein. However, the highest fluctuations were experienced by the residues numbered 191, 231 and $266-291$, which are less participating in the active binding of the receptor. The results also support higher conformational stability of the ligands **Amb35813946** and **Amb18709727** than **Amb37857532** and **Amb932777** as well as **lorpiprazole** in complex with the receptor, consistently with the RMSD plot.

The interactive contacts of the selected NβCs, as well as lorpiprazole with the amino acid residues in the active binding pocket of the 5-HT1A receptor, are indicated by the contact charts (Figure 7). These protein-ligand interactions were expressed as hydrogen bonds, hydrophobic, ionic and water bridges. Generally, all the selected ligands as well as the reference **lorpiprazole** exhibited strong water-mediated hydrogen bond interactions with residues Asp 116, Ile 189 and Asn 386, consistently with previous results (Figure 3). This importantly supports their strong inhibitory binding potentials against the receptor, and pharmacological profiles for

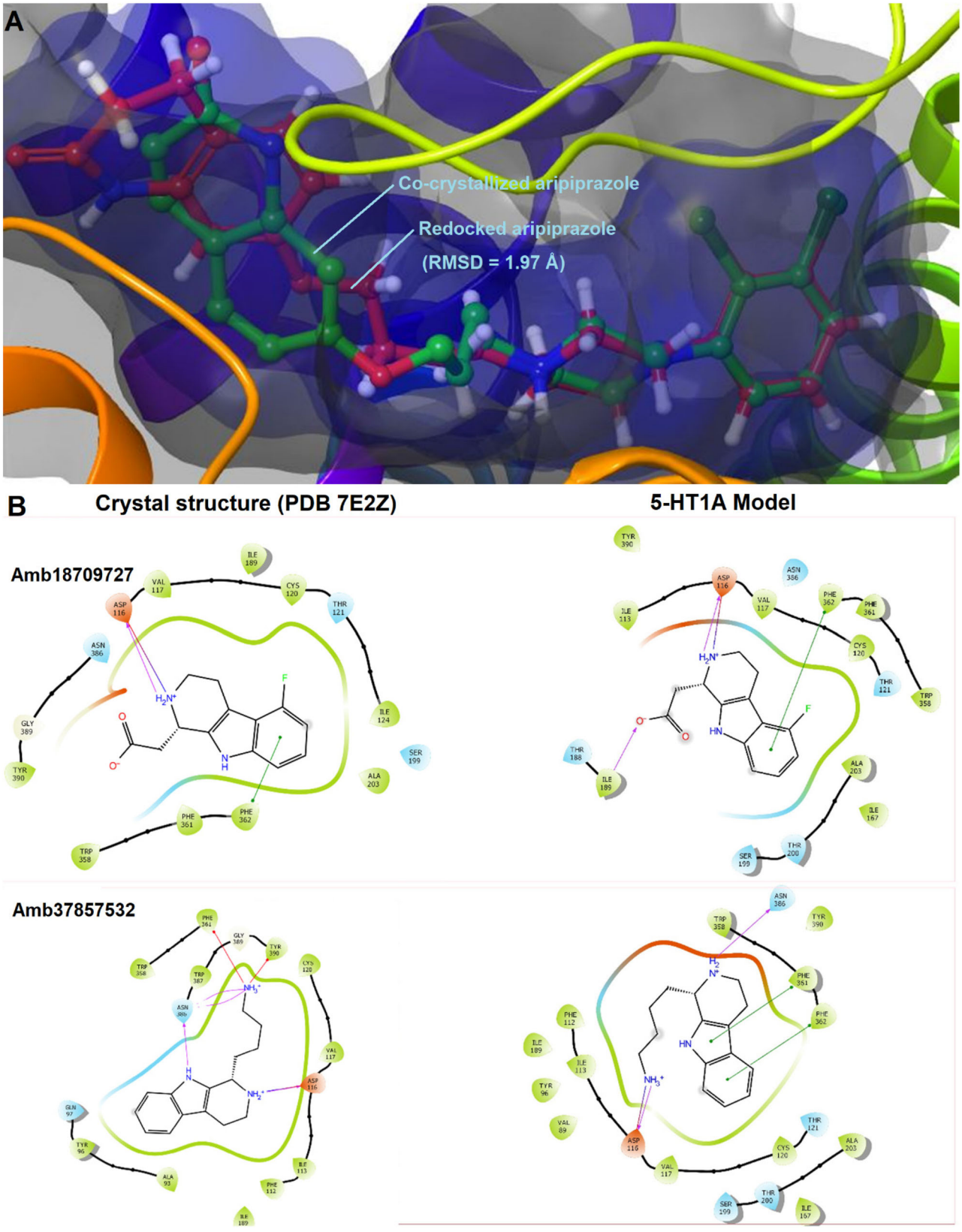


Figure 3. Revalidation of docking protocols. (A) 3 D Binding pose of co-crystallized and redocked aripiprazole superimposed at the active binding pocket of PDB 7E2Z. Ball and stick model: co-crystallized aripiprazole (green); redocked aripiprazole (red); RMSD = 1.97 Ð (B) 2 D Binding poses of **Amb18709727** and **Amb37857532** with the crystal structure of 5-HT1A receptor (PDB 7E2Z) and model 5-HT1A receptor. Similar active pocket residues and binding interactions displayed support a good resemblance between the modelled receptor and the crystal structure.

absorption, metabolism and specificity. They also expressed a good number of hydrophobic and water bridges but few ionic interactions. Consistently with the previous results, ligands **Amb35813946** and **Amb18709727** displayed the highest number of contacts with the active amino acid residues while **lorpiprazole** showed no ionic interactions.

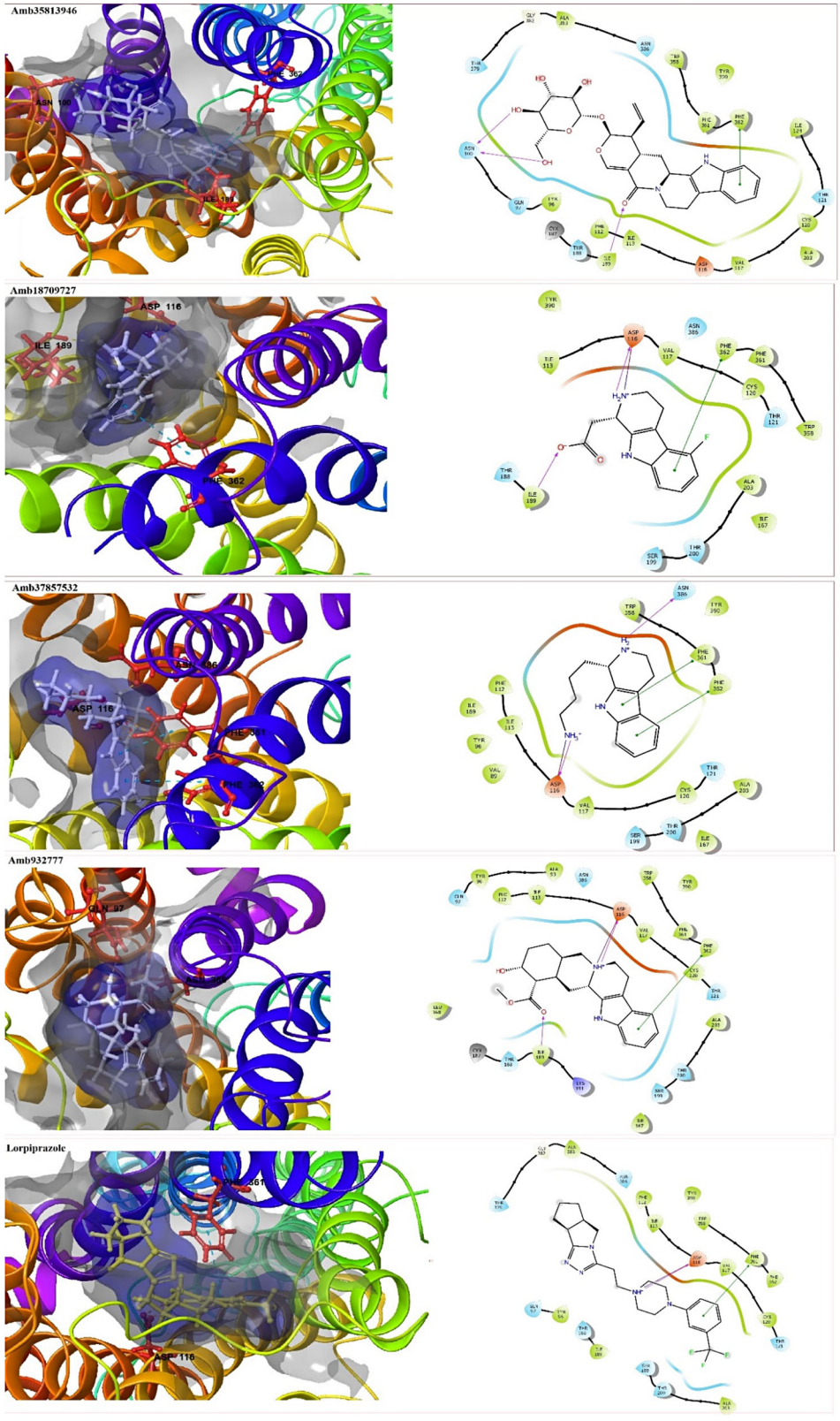


Figure 4. Binding poses illustrating the interactions between the selected NβC ligands and amino acid residues in the active pocket of the 5-HT1A homology receptor compared to reference drug. (Left) 3 D illustration of the ligand interactions at the active binding pocket (blue and grey solid region). Ball and stick models: Selected ligands (white), lorpiprazole reference ligand (yellow), interactive bonding amino acid residues (red). (Right) 2 D illustration of the bonding and non-bonding ligand interactions with amino acid residues (small circles). Polar residues (blue), hydrophobic residues (yellow), negatively charged residues (red), positively charged residues (indigo), unspecified residues (grey). Bonding interactions: H-bond (magenta arrow), salt-bridge (red-blue line), π-π stacking (green line), π-cation (red line). The selected ligands showed more bonding interactions than lorpiprazole, indicating higher inhibitory interactions.

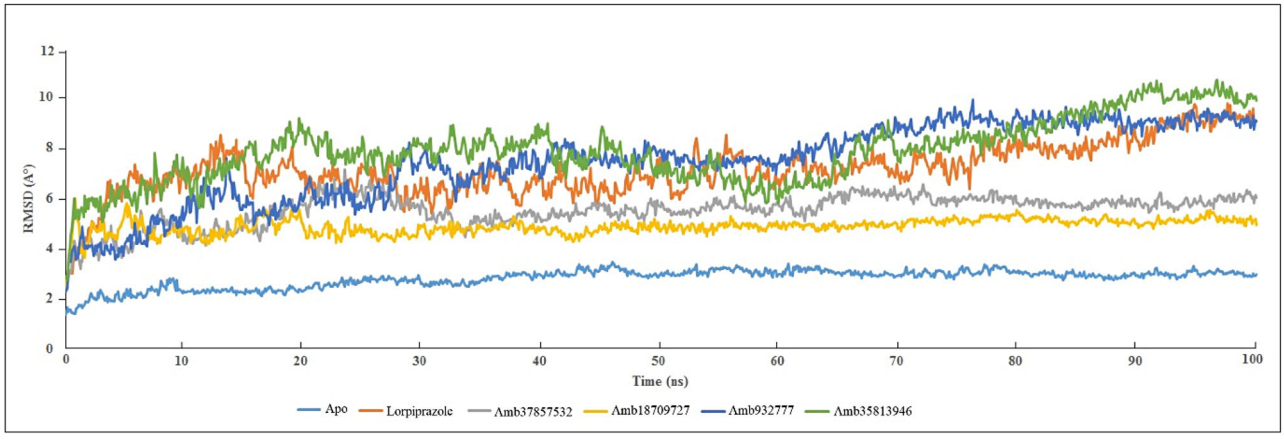


Figure 5. Time-dependent RMSD during 100 ns MD simulations of the Apo protein backbone, selected NβC ligands and reference lorpiprazole. The Apo protein backbone attained equilibrium within the first 5 seconds of simulation and maintained good stability with an average fluctuation of ≈1.5 Ð throughout the simulation period. Although, all the selected ligands including **lorpiprazole** showed good contacts with the protein backbone throughout the 100 ns simulation. However, ligands, **Amb37857532** and **Amb18709727** impressively attained equilibrium around 10 ns and maintained a good stability with an average fluctuation of <2.0 Ð throughout the simulation, indicating better stability with the receptor than others.

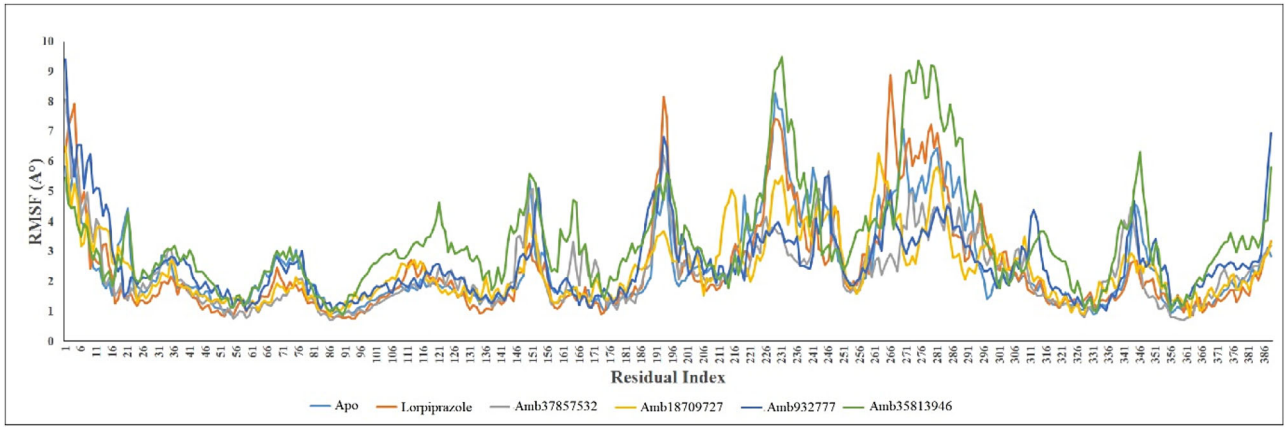


Figure 6. RMSF plot of the selected NβC ligands and reference lorpiprazole. Lower fluctuations are also demonstrated by the selected NβC ligands, especially **Amb37857532** and **Amb18709727** inferring higher stability than others including **lorpiprazole**. Interestingly, the two ligands improve the stability of the highly unstable residues such as the residues with number 191, 231 and 276 during the contacts.

The 2 D intermolecular interaction diagrams from the MD simulation (Figure 8) reveals more detailed interactions between the selected NβC and the active site amino acid residues of the 5-HT1A receptor, which could not be observed from the molecular docking poses. The additional interactions such as the water-mediated H-bonds to Lys 191, Asn 386 and hydrophobic through Tyr 96 by **Amb18709727** and water-mediated H-bond to Gly 382 and ionic participation to Phe 112 by **Amb37857532** support the higher binding affinities, thermodynamic stabilities and more ideal flexibility of the two NβC ligands. The cumulative observations from the virtual screening to MD molecular simulations indicate that the ligands, **Amb18709727** and **Amb37857532** excellently display stronger inhibitory potentials and better stabilities than others including the reference lorpiprazole. As such, the two ligands were selected for further *in silico* study on ADMET properties.

Binding free energy (MMGBSA) calculation

The post simulation MM-GBSA analysis of binding free energy (ΔG_{Bind}) calculation was carried out with the generation of 500-1001 frames having a 100-step sampling size. A total of 6 frames were processed and analysed throughout the 100 ns MD data of the lead compounds. From Table 2, the binding free energy (MMGBSA) values of the ligands, **Amb18709727** and **Amb37857532** are −87.972 and −107.585 kcal/mol respectively while that of **Lorpiprazole** is estimated as −62.780 kcal/mol. This indicates stronger bindings and inhibitory potentials consistently with docking scores (Zrieq et al., 2021).

In silico pharmacokinetics, pharmacodynamics and druggability

The physicochemical parameters which inclusively dictate the pharmacokinetics, pharmacodynamics and druggability profiles of the four selected NβC alkaloids are presented in Table 3. The initial estimation has been reported to reliably reduce pharmacokinetic failures of potential drug molecules upon further investigation (Daina et al., 2017). From the results obtained from the server (Daina et al., 2017), the selected ligands, **Amb18709727** and **Amb37857532** have MW in the range of 150 − 500 g/mol, <10 HBA, <5 HBD, TPSA 20 − 130 Å^2, XLog

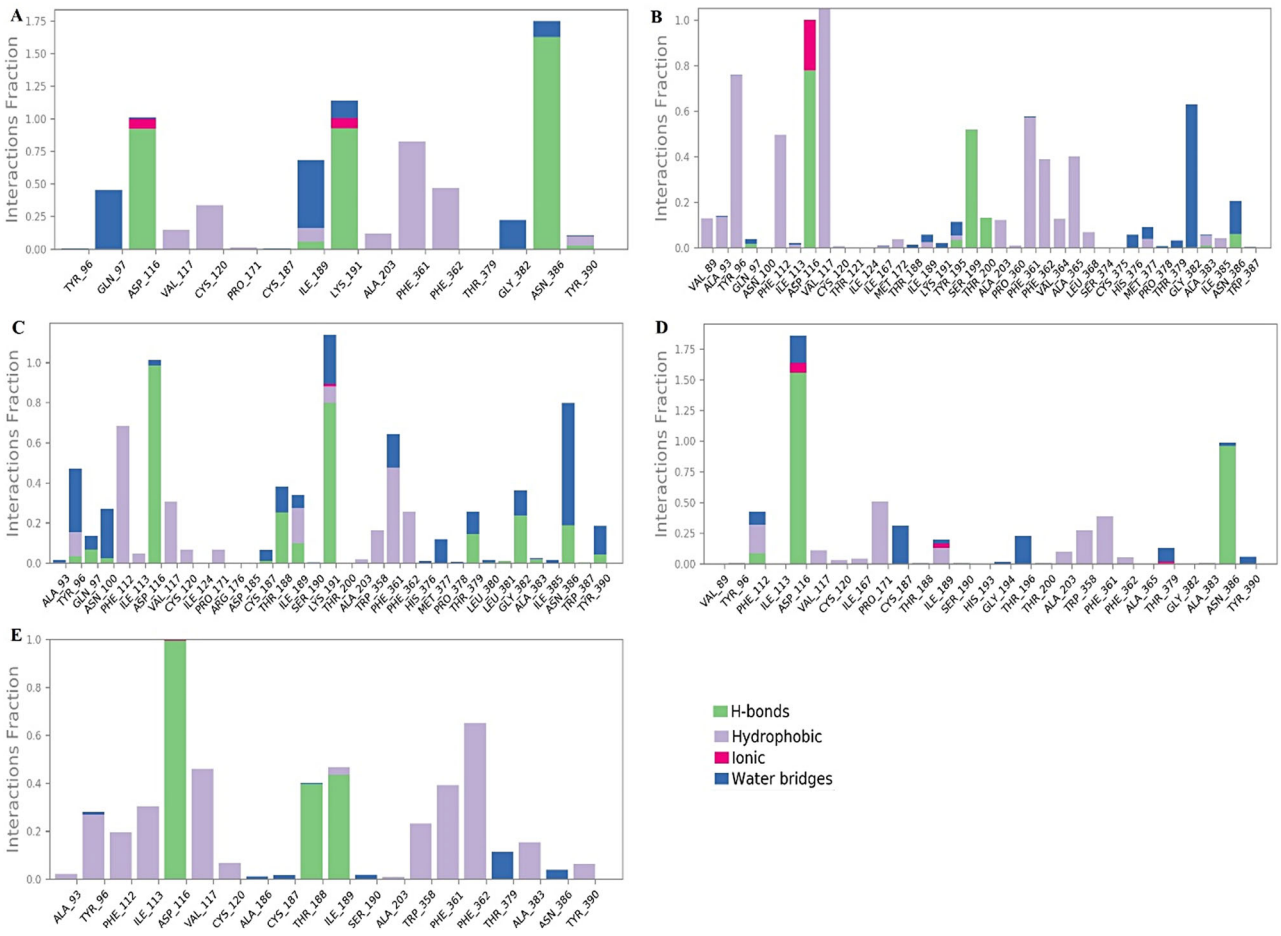


Figure 7. Charts showing contacts between selected ligands and the interactive residues of 5-HT1A receptor (A) **Amb35813946** (B) **Amb18709727** (C) **Amb37857532** (D) **Amb932777** (E) **Lorpiprazole**. The ligands, **Amb37857532** and **Amb18709727** consistently have interactive contacts with more amino acid residues than others, supporting their higher binding affinities.

P3 within −0.7 - +5.0, the fraction of sp3 carbon ≥0.25 and Log S < 6. They all possess strong abilities to cross main biological barriers such as the gastrointestinal absorption (GI) for oral bioavailability and blood-brain barrier (BBB) for brain access, consistently with the known medication, **lorpiprazole**. Also, as shown in the bioavailability radar (Figure 9), the selected ligands have ideal enzymatic stability, flexibility, lipophilicity (affinity for efflux mechanisms), size, solubility, saturation and polarity (within the pink hexagons) as expected of promising candidates. These physicochemical, pharmacokinetics and pharmacodynamics qualitatively fall within the required standards for molecules with the propensity for lead-like drug candidates and medicinal suitability for homeostatic processes in the central nervous system (CNS) (Daina et al., 2017; Meairs, 2015; Pajouhesh & Lenz, 2005).

In silico toxicology and mutagenicity

Having satisfied the physiochemical, pharmacokinetics and pharmacodynamics requirements to be considered as CNS drug-like candidates, other important determinants of their medicinal suitability of the selected ligands, **Amb18709727** and **Amb37857532** especially as SARI antidepressants include toxicological and mutagenic expressions for side effects. According to Daina et al., P-glycoprotein (P-gp) substrates protect the CNS from xenobiotics (Daina et al., 2017). From Table 3, the two selected NβCs, **Amb18709727** and **Amb37857532** displayed expressions for good P-gp substrates, indicating a tendency for not accumulating in the CNS whereas, trazodone, a popular SARI antidepressant fails in this prospect. The inhibition of the cytochrome P450 (CYP) superfamily isoenzymes (CYPs 1A2, 2C19, 2C9, 2D6 and 3A4) by drug molecules mainly constitute the unwanted pharmacokinetics-related drug interactions. These interactions often induce drug elimination within biological systems through metabolic transformations (Daina et al., 2017). Overall, the selected ligands show no inhibitory expressions against the CYPs except 2D6, similarly to the reference drugs. Although, the metabolic expression of CYP2D6 is commonly observed in lipophilic amines, however, **Amb18709727** considerably tend to be exceptionally safer than lorpiprazole and trazodone even in this regard. The inhibition of CYPs 1A2 and 3A4 beleaguers the therapeutic indices of most antidepressant and antipsychotic drugs including lorpiprazole, a reference SARI drug in this study (Mitchell, 2004, 2020). The two selected NβC alkaloids, **Amb18709727** and **Amb37857532** also demonstrated potentials to be exceptionally non-inhibitors of CYPs 1A2 and 3A4. Their highly negative Log Kp values indicate a lower chance for skin permeation (Daina et al., 2017) consistently with the positive antidepressant references. They showed no violation to both Lipinski's and

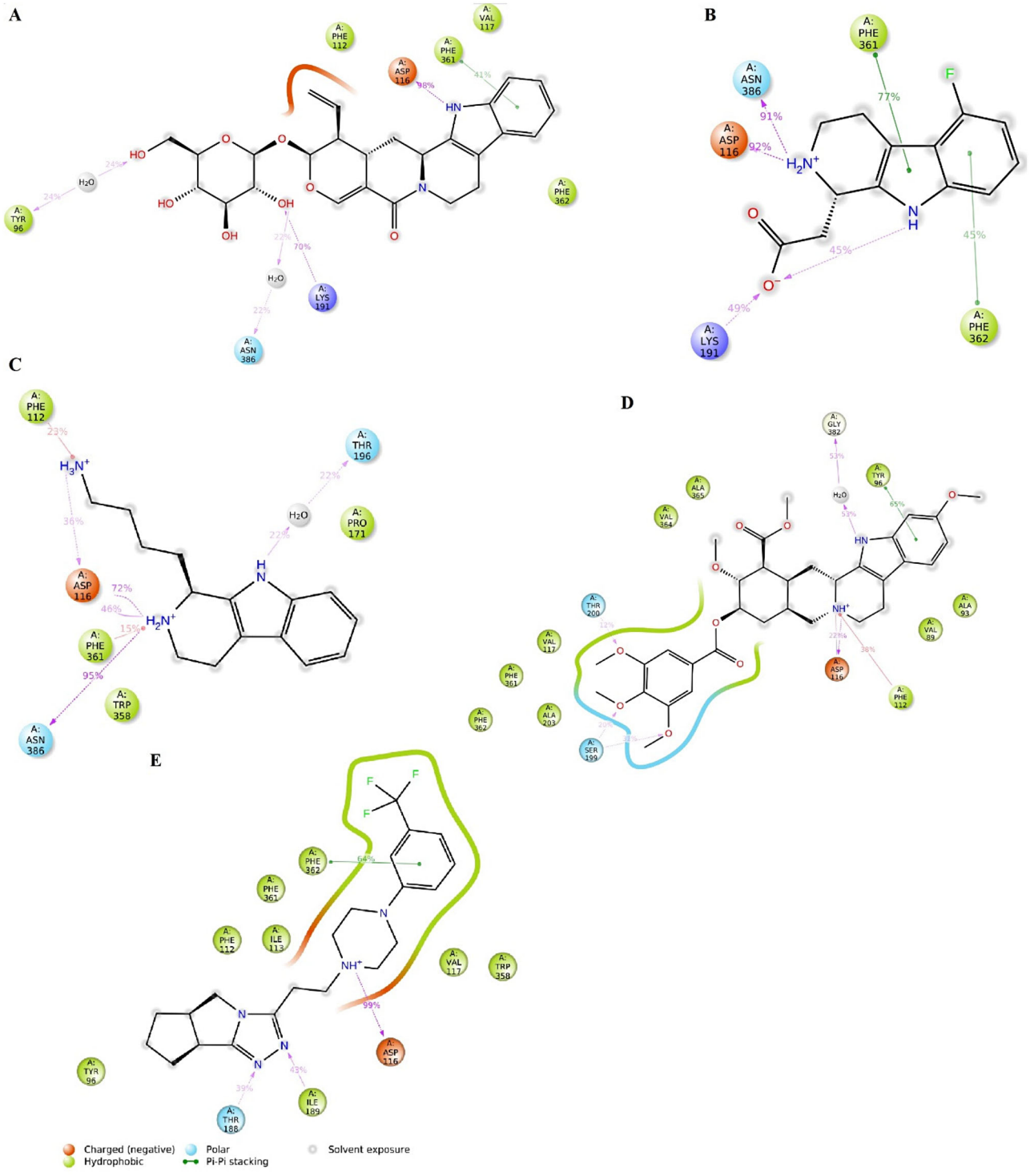


Figure 8. 2 D Intermolecular interactions of the selected ligands with active residues of the 5-HT1A receptor. The ligands, **Amb37857532** and **Amb18709727** interacted more potently with active amino acid residues of 5-HT1A receptor than others including lorpiprazole.

BDDC's rules of 5 for drugability (Benet et al., 2016; Lipinski, 2004), insignificant PAIN alerts, good bioavailability (Figure 9A) and synthetic accessibility scores, thus, represent promising and accessible lead-like SARI candidates upon further experimental assessments.

The mutagenicity potential of a chemical molecule to cause genetic mutations remains a major public health concern for its druggability. The undesired biochemistry is evaluated *in silico* for the selected compounds to further confirm their safety compared to the reference drugs using VEGA ToxRead Java-based software. The mutagenicity results from a read-across SAR of the selected ligands about fragment search and similarity measures to relevant molecules are represented by Figure 9B. The middle circle represents the molecule being studied while the colour indicates expression for mutagenicity: non-mutagenic (green), mutagenic (red) (Y.O. Ayipo et al., 2021; Gini et al., 2014). It could be observed that the four selected NβC alkaloids displayed non-mutagenicity, consistently with lorpiprazole. This also supports their relative safety compared to the commonly prescribed SARIs.

Table 3. Pharmacokinetics, pharmacodynamics and druggability of the selected NβC ligands.

Molecule	Amb18709727	Amb37857532	Lorpiprazole	Trazodone
Molecular weight (g/mol)	248.25	243.35	405.46	371.86
#Hydrogen bond acceptor	4	2	6	3
#Hydrogen bond donor	3	3	0	0
#Rotatable bonds	2	4	5	5
Fraction Csp3	0.31	0.47	0.62	0.37
TPSA (Å^2)	65.12	53.84	37.19	45.78
XLog P3	−1.16	1.65	3.32	2.84
ESOL Log S	−0.89	−2.49	−4.4	−4.03
GI absorption	High	High	High	High
BBB	Yes	Yes	Yes	Yes
P-gp substrate	Yes	Yes	Yes	No
CYP1A2 inhibition	No	No	No	No
CYP2C19 inhibition	No	No	No	No
CYP2C9 inhibition	No	No	No	Yes
CYP2D6 inhibition	No	Yes	Yes	Yes
CYP3A4 inhibition	No	No	Yes	No
Log Kp (cm/s)	−8.64	−6.61	−6.42	−6.55
Lipinski violation	0	0	0	0
Bioavailability	0.55	0.55	0.55	0.55
PAINS alerts	0	1	0	0
Synthetic accessibility	2.84	2.84	4.12	2.93

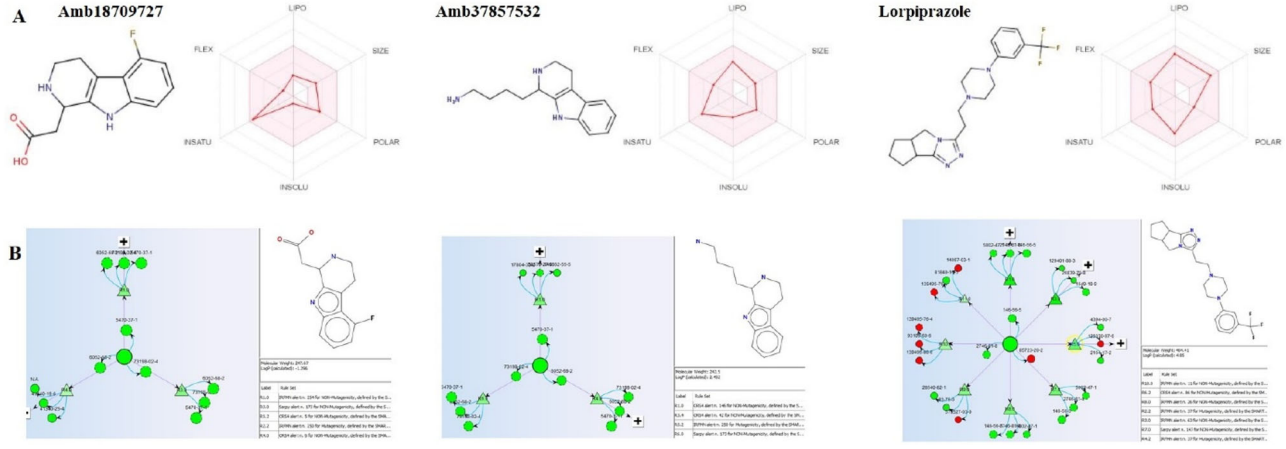
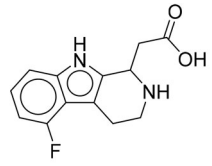
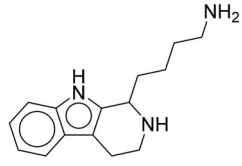


Figure 9. Bioavailability and mutagenicity radars of the selected NβC alkaloids in comparison with the reference lorpiprazole. (A) Bioavailability illustration of the ideal drug-like profiles of **Amb18709727** and **Amb37857532**, in strong similarity to **Lorpiprazole**. (B) Read-across mutagenicity radar indicating lesser mutagenic potentials of **Amb18709727** and **Amb37857532** (no red circles) compared to **Lorpiprazole** (with some red circles).



2-(5-fluoro-2,3,4,9-tetrahydro-1*H*-pyrido[3,4-*b*]indol-1-yl)acetic acid

Amb18709727



4-(2,3,4,9-tetrahydro-1*H*-pyrido[3,4-*b*]indol-1-yl)butan-1-amine

Amb37857532

Figure 10. Chemical structures of the four NβC alkaloids with promising SARI ligands.

Final hits

Two NβC alkaloids, **Amb18709727** and **Amb37857532** (Figure 10) represent the final hit. They demonstrated stronger potentials for antagonism and inhibition of 5-HT1A than reference SARI antidepressants, lorpiprazole and trazodone. They also showed more interesting physicochemical, pharmacokinetics and pharmacodynamics (ADME) properties relevant to the medicinal application as SARIs than the reference drugs. They are commercially available at Ambinter-Greenpharma chemical library and possess good synthetic accessibility, although **Amb37857532** is reportedly present in a measurable amount in *Nitraria schoberi* (Wink, 2000). Significantly, they displayed lower expression for CYP isoenzymes inhibition and non-mutagenicity than the reference drugs. Similar virtual screening studies have also been reported in favour of some selected hits with equal or lesser predicted toxicological parameters than approved drugs through similar media (Abu-Melha et al., 2022; Durán-Iturbide et al., 2020; Umar et al., 2020). Further wet-lab biochemical analyses are required to affirm the theoretical findings. The results obtained in this study are in agreement

with those deduced for coumarin derivatives, which were later confirmed as potent 5-HT1A antagonists and inhibitors upon biochemical experiments (K. Ostrowska et al., 2017; Ostrowska et al., 2018). The consistency in the findings and analogy from previous studies constitute strong confidence and pose the compounds as promising SARI candidates from vast natural products with enhanced pharmacological potentials and lower expressions for side effects amenable for further translational studies.

Conclusions

The application of computer-aided drug design has led to the discovery of several drug molecules with successful medicinal applications. In this study, two ligands with the database annotations, **Amb18709727** and **Amb37857532** respectively demonstrated stronger inhibitory and antagonistic potentials against 5-HT1A receptor than **lorpiprazole** and **trazodone**, referenced SARI antidepressants. They displayed enhanced stability and compactness with the human 5-HT1A receptor than lorpiprazole. They showed interesting physicochemical, pharmacokinetics and pharmacodynamic potentials for enhanced pharmacology and medicinal implications, and toxicological propensity for lesser side effects. Moreover, the available information shows that the two selected NβC alkaloids have not been reported as 5-HT1A antagonists and reuptake inhibitors, supporting their novelty for further exploration. Although, basic and clinical experimental studies through target-based *in vitro* and animal-based *in vivo* models are required to further authenticate the promising enhanced pharmacology and lower potentials for side effects as revealed in this theoretical investigation. However, the cumulative findings build confidence for embarking on such rigorous and resource-demanding scientific evaluation to translate the selected ligands into real-life therapeutics. The study represents a cost-effective, faster and environmentally friendly model for the identification of lead-like SARI potentials from vast natural products amenable for further study. The finally retrieved hits are promising SARI candidates recommended for experimental assessments.

Disclosure statement

No potential conflict of interest was reported by the author(s).

Funding

This work was supported by Tertiary Education Fund Nigeria, Fundamental Research Grant Scheme (203.CDADAH.6711955), Ministry of Higher Education of Malaysia and Universiti Sains Malaysia GA Scheme (grant no. 308.AIPS.415401).

ORCID

Yusuf Oloruntoyin Ayipo http://orcid.org/0000-0001-5951-9788
Waleed A. Alananzeh http://orcid.org/0000-0003-3173-1132
Iqrar Ahmad http://orcid.org/0000-0002-7697-9572
Harun Patel http://orcid.org/0000-0003-0920-1266
Mohd Nizam Mordi http://orcid.org/0000-0002-0997-3867

References

Abu-Melha, S., Edrees, M. M., Said, M. A., Riyadh, S. M., Al-Kaff, N. S., & Gomha, S. M. (2022). Potential COVID-19 drug candidates based on diazinyl-thiazol-imine moieties: Synthesis and greener pastures biological study. *Molecules*, *27*(2), 488. https://doi.org/10.3390/molecules27020488

Ahmad, I., Jadhav, H., Shinde, Y., Jagtap, V., Girase, R., & Patel, H. (2021). Optimizing Bedaquiline for cardiotoxicity by structure based virtual screening, DFT analysis and molecular dynamic simulation studies to identify selective MDR-TB inhibitors. *In Silico Pharmacology*, *9*(1), 23. https://doi.org/10.1007/s40203-021-00086-x

Ahmad, I., Kumar, D., & Patel, H. (2021). Computational investigation of phytochemicals from Withania somnifera (Indian ginseng/ashwagandha) as plausible inhibitors of GluN2B- containing NMDA receptors Computational investigation of phytochemicals from Withania somnifera (Indian ginseng/as. *Journal of Biomolecular Structure and Dynamics*, 1–13. https://doi.org/10.1080/07391102.2021.1905553

Ayipo, Y. O., Alananzeh, W. A., Yahaya, S. N., & Mordi, M. N. (2022). Molecular modelling and virtual screening to identify new piperazine derivatives as potent human 5-HT1A antagonists and reuptake inhibitors. *Combinatorial Chemistry and High Throughput Screening*, *25*, 1–20.

Ayipo, Y. O., Mordi, M. N., Mustapha, M., & Damodaran, T. (2021). Neuropharmacological potentials of β-carboline alkaloids for neuropsychiatric disorders. *European Journal of Pharmacology*, *893*, 173837. https://doi.org/10.1016/j.ejphar.2020.173837

Ayipo, Y. O., Osunniran, W. A., & Mordi, M. N. (2021). Metal complexes of β-carboline: Advances in anticancer therapeutics. *Coordination Chemistry Reviews*, *432*, 213746. https://doi.org/10.1016/j.ccr.2020.213746

Ayipo, Y. O., Yahaya, S. N., Babamale, H. F., Ahmad, I., Patel, H., & Mordi, M. N. (2021). β-Carboline alkaloids induce structural plasticity and inhibition of SARS-CoV-2 nsp3 macrodomain more potently than remdesivir metabolite GS-441524: Computational approach. *Turkish Journal of Biology*, *45*(SI-1), 503–517. https://doi.org/10.3906/biy-2106-64

Benet, L. Z., Hosey, C. M., Ursu, O., Oprea, T. I., Sciences, T., & Division, I. (2016). BDDCS, the rule of 5 and drugability leslie. *Advanced Drug Delivery Reviews*, *101*, 89–98. https://doi.org/10.1016/j.addr.2016.05.007.BDDCS

Blei, A. F., Dörner, S., Fricke, J., Baldeweg, F., Trottmann, F., Komor, A., Meyer, F., & Hoffmeister, D. (2019). Simultaneous production of psilocybin and a cocktail of β- carboline monoamine oxidase inhibitors in "magic" mushrooms. *Chemistry - A European Journal*, *26*, 729–734. https://doi.org/10.1002/chem.201904363

Castro-Alvarez, A., Costa, A. M., & Vilarrasa, J. (2017). The performance of several docking programs at reproducing protein-macrolide-like crystal structures. *Molecules*, *22*(1), 136. https://doi.org/10.3390/molecules22010136

Colovos, C., & Yeates, T. (1993). Verification of protein structures: Patterns of nonbonded atomic interactions. *Protein Science: A Publication of the Protein Society*, *2*(9), 1511–1519. https://doi.org/10.1002/pro.5560020916

Cui, Y., Shen, N., Dang, J., Mei, L., Tao, Y., & Liu, Z. (2017). Anti-inflammatory bioactive equivalence of combinatorial components β-carboline alkaloids identified in Arenaria Kansuensis by two-dimensional chromatography and solid-phase extraction coupled with liquid–liquid extraction enrichment technology. *Journal of Separation Science*, *40*(14), 2895–2905. https://doi.org/10.1002/jssc.201700144

D. E. Shaw Research. (2021). *Maestro-desmond interoperability tools, Schrödinger release 2020-3, New York, NY, 2020. (Schrodinger release 2020-3)*. Schrodinger.

Dai, J., Dan, W., Schneider, U., & Wang, J. (2018). β-Carboline alkaloid monomers and dimers: Occurrence, structural diversity, and biological activities. *European Journal of Medicinal Chemistry*, *157*, 622–656. https://doi.org/10.1016/j.ejmech.2018.08.027

Daina, A., Michielin, O., & Zoete, V. (2017). SwissADME: A free web tool to evaluate pharmacokinetics, drug-likeness and medicinal chemistry friendliness of small molecules. *Scientific Reports*, *7*, 42717. https://doi.org/10.1038/srep42717

Durán-Iturbide, N. A., Díaz-Eufracio, B. I., & Medina-Franco, J. L. (2020). In Silico ADME/Tox profiling of natural products: A focus on

BIOFACQUIM. *ACS Omega*, *5*(26), 16076–16084. https://doi.org/10.1021/acsomega.0c01581

Dyson, H. J., Wright, P. E., & Scheraga, H. A. (2006). The role of hydrophobic interactions in initiation and propagation of protein folding. *Proceedings of the National Academy of Sciences of the United States of America*, *103*(35), 13057–13061. https://doi.org/10.1073/pnas.0605504103

Fasipe, O. J. (2018). Neuropharmacological classification of antidepressant agents based on their mechanisms of action. *Archives of Medicine and Health Sciences*, *6*(1), 81–94. https://doi.org/10.4103/amhs.amhs_7_18

Ferraz, C. A. A., de Oliveira Júnior, R. G., Picot, L., da Silva Almeida, J. R. G., & Nunes, X. P. (2019). Pre-clinical investigations of β-carboline alkaloids as antidepressant agents: A systematic review. *Fitoterapia*, *137*(May), 104196. https://doi.org/10.1016/j.fitote.2019.104196

Forouzesh, N., & Mishra, N. (2021). An effective MM/GBSA protocol for absolute binding free. *Molecules*, *26*(8), 2383. https://doi.org/10.3390/molecules26082383

Genheden, S., & Ryde, U. (2015). The MM/PBSA and MM/GBSA methods to estimate ligand-binding affinities. *Expert Opinion on Drug Discovery*, *10*(5), 449. https://doi.org/10.1517/17460441.2015.1032936

Gini, G., Franchi, A. M., Manganaro, A., Golbamaki, A., & Benfenati, E. (2014). ToxRead: A tool to assist in read across and its use to assess mutagenicity of chemicals. *SAR and QSAR in Environmental Research*, *25*(12), 999–1011. https://doi.org/10.1080/1062936X.2014.976267

Halgren, T. (2009). Identifying and characterizing binding sites and assessing druggability. *Journal of Chemical Information and Modeling*, *49*(2), 377–389. https://doi.org/10.1021/ci800324m

Halgren, T. A., Murphy, R. B., Friesner, R. A., Beard, H. S., Frye, L. L., Pollard, W. T., & Banks, J. L. (2004). Glide: A new approach for rapid, accurate docking and scoring. 2. Enrichment factors in database screening. *Journal of Medicinal Chemistry*, *47*(7), 1750–1759. https://doi.org/10.1021/jm030644s

Harder, E., Damm, W., Maple, J., Wu, C., Reboul, M., Xiang, J. Y., Wang, L., Lupyan, D., Dahlgren, M. K., Knight, J. L., Kaus, J. W., Cerutti, D. S., Krilov, G., Jorgensen, W. L., Abel, R., & Friesner, R. A. (2016). OPLS3: A force field providing broad coverage of drug-like small molecules and proteins. *Journal of Chemical Theory and Computation*, *12*(1), 281–296. https://doi.org/10.1021/acs.jctc.5b00864

Hooft, R. W., Vriend, G., Sander, C., & Abola, E. E. (1996). Errors in protein structures. *Nature*, *381*(6580), 272. https://doi.org/10.1038/381272a0

Ibrahim, S. R. M., & Mohamed, G. A. (2017). Ingenine E, a new cytotoxic β-carboline alkaloid from the Indonesian sponge Acanthostrongylophora ingens. *Journal of Asian Natural Products Research*, *19*(5), 504–506. https://doi.org/10.1080/10286020.2016.1213723

Jaffer, K. Y., Chang, T., Vanle, B., Dang, J., Steiner, A. J., Loera, N., Abdelmesseh, M., Danovitch, I., & Ishak, W. W. (2017). Trazodone for insomnia: A systematic review. *Innovations in Clinical Neuroscience*, *14*(7-8), 24–34.

Jorgensen, W. L., Maxwell, D. S., & Tirado-rives, J. (1996). Development and testing of the OPLS all-atom force field on conformational energetics and properties of organic liquids. *Journal of the American Chemical Society*, *118*(45), 11225–11236. https://doi.org/10.1021/ja9621760

Karim, N., Khan, I., Abdelhalim, A., Khan, A., & Halim, S. A. (2018). Antidepressant potential of novel flavonoids derivatives from sweet violet (Viola odorata L): Pharmacological, biochemical and computational evidences for possible involvement of serotonergic mechanism. *Fitoterapia*, *128*(April), 148–161. https://doi.org/10.1016/j.fitote.2018.05.016

Kochanowska-Karamyan, A. J., Araujo, H. C., Zhang, X., El-Alfy, A., Carvalho, P., Avery, M. A., Holmbo, S. D., Magolan, J., & Hamann, M. T. (2020). Isolation and synthesis of veranamine, an antidepressant lead from the marine sponge verongula rigida. *Journal of Natural Products*, *83*(4), 1092–1098. https://doi.org/10.1021/acs.jnatprod.9b01107

Krystal, A. D. (2013). Pharmacologic treatment of insomnia: Other medications. In *Encyclopedia of sleep* (6th ed., pp. 842–854). Elsevier Inc. https://doi.org/10.1016/B978-0-12-378610-4.00200-X

Lipinski, C. A. (2004). Lead- and drug-like compounds: The rule-of-five revolution. *Drug Discovery Today. Technologies*, *1*(4), 337–341. https://doi.org/10.1016/j.ddtec.2004.11.007

Luthy, R., Bowie, J. U., & Eisenberg, D. (1992). Assessment of protein modes with three-dimensional profiles. *Nature*, *356*(6364), 83–85. https://doi.org/10.1038/356083a0

Madhavi Sastry, G., Adzhigirey, M., Day, T., Annabhimoju, R., & Sherman, W. (2013). Protein and ligand preparation: Parameters, protocols, and influence on virtual screening enrichments. *Journal of Computer-Aided Molecular Design*, *27*(3), 221–234. https://doi.org/10.1007/s10822-013-9644-8

Marondedze, E. F., Govender, K. K., & Govender, P. P. (2020). Computational investigation of the binding characteristics of β-amyloid fibrils. *Biophysical Chemistry*, *256*, 106281. https://doi.org/10.1016/j.bpc.2019.106281

Meairs, S. (2015). Facilitation of drug transport across the blood–brain barrier with ultrasound and microbubbles. *Pharmaceutics*, *7*(3), 275–293. https://doi.org/10.3390/pharmaceutics7030275

Mitchell, P. B. (2004). Therapeutic drug monitoring of antidepressant and antipsychotic drugs. In G. Hempel (Ed.), *Drug monitoring and clinical chemistry: Handbook of analytical separations* (Vol. 5, pp. 269–271). Elsevier B. V. https://doi.org/10.1016/S1567-7192(04)80011-1

Mitchell, P. B. (2020). Therapeutic drug monitoring of antidepressant and antipsychotic drugs. In *Methods of therapeutic drug monitoring including pharmacogenetics* (Vol. *7*, pp. 257–275). Elsevier. https://doi.org/10.1016/B978-0-444-64066-6.00011-3

Mohankumar, T., Chandramohan, V., Lalithamba, H. S., Jayaraj, R. L., Kumaradhas, P., Sivanandam, M., Hunday, G., Vijayakumar, R., Balakrishnan, R., Manimaran, D., & Elangovan, N. (2020). Design and molecular dynamic investigations of as potential neuroprotective agents against alpha-synuclein. *Scientific Reports*, *10*(1), 599. https://doi.org/10.1038/s41598-020-57417-9

Negi, A., Reilly, C. O., Jarikote, D. V., Zhou, J., & Murphy, P. V. (2019). Multi-targeting protein-protein interaction inhibitors: Evolution of macrocyclic ligands with embedded carbohydrates (MECs) to improve selectivity. *European Journal of Medicinal Chemistry*, *176*, 292–309. https://doi.org/10.1016/j.ejmech.2019.04.064

Nosé, S. (1984). A unified formulation of the constant temperature molecular dynamics. *The Journal of Chemical Physics*, *81*(1), 511–519. https://doi.org/10.1063/1.447334

Ostrowska, K., Grzeszczuk, D., Głuch-Lutwin, M., Gryboś, A., Siwek, A., Dobrzycki, Ł., & Trzaskowski, B. (2017). Development of selective agents targeting serotonin 5HT1A receptors with subnanomolar activities based on a coumarin core. *MedChemComm*, *8*(8), 1690–1696. https://doi.org/10.1039/C7MD00281E

Ostrowska, K., Grzeszczuk, D., Głuch-Lutwin, M., Gryboś, A., Siwek, A., Leśniak, A., Sacharczuk, M., & Trzaskowski, B. (2018). 5-HT1A and 5-HT2A receptors affinity, docking studies and pharmacological evaluation of a series of 8-acetyl-7-hydroxy-4-methylcoumarin derivatives. *Bioorganic & Medicinal Chemistry*, *26*(2), 527–535. https://doi.org/10.1016/j.bmc.2017.12.016

Pajouhesh, H., & Lenz, G. R. (2005). Medicinal chemical properties of successful central nervous system drugs. *NeuroRX*, *2*(4), 541–553. https://doi.org/10.1602/neurorx.2.4.541

Patel, H. M., Shaikh, M., Ahmad, I., Lokwani, D., & Sanjay, J. (2021). BREED based de novo hybridization approach: generating novel T790M/C797S-EGFR tyrosine kinase inhibitors to overcome the problem of mutation and resistance in non small cell lung cancer (NSCLC). *Journal of Biomolecular Structure & Dynamics*, *39*(8), 2838–2856. https://doi.org/10.1080/07391102.2020.1754918

Phillips, M. A., Stewart, M. A., Woodling, D. L., & Xie, Z.-R. (2018). Has molecular docking docking ever ever brought brought us us a a medicine? In *Molecular dockingocking* (pp. 141–178). IntechOpen. https://doi.org/10.5772/intechopen.72898

Pontius, J., Richelle, J., & Wodak, S. J. (1996). Deviations from standard atomic volumes as a quality measure for protein crystal structures. *Journal of Molecular Biology*, *264*(1), 121–136. https://doi.org/10.1006/jmbi.1996.0628

Prandi, A., Franchini, S., Manasieva, L. I., Fossa, P., Cichero, E., Marucci, G., Buccioni, M., Cilia, A., Pirona, L., Brasili, L., Farmaceutiche, S., Emilia, R., & Campi, V. (2012). Synthesis, biological evaluation, and docking studies of tetrahydrofuran- cyclopentanone- and cyclopentanol-based ligands acting at adrenergic α 1 - and serotonine 5-HT 1A receptors. *Journal of Medicinal Chemistry*, *55*(1), 23–36. https://doi.org/10.1021/jm200421e

Ramírez, D., & Caballero, J. (2018). Is it reliable to take the molecular docking top scoring position as the best solution without considering available structural data? *Molecules*, *23*(5), 1038. https://doi.org/10.3390/molecules23051038

Sun, H., Duan, L., Chen, F., Liu, H., Wang, Z., Pan, P., Zhu, F., Zhang, J. Z. H., & Hou, T. (2018). Assessing the performance of MM/PBSA and MM/GBSA methods. 7. Entropy effects on the performance of end-point binding free energy calculation approaches. *Physical Chemistry Chemical Physics: PCCP*, *20*(21), 14450–14460. https://doi.org/10.1039/c7cp07623a

Taciak, P. P., Lysenko, N., & Mazurek, A. P. (2018). Drugs which influence serotonin transporter and serotonergic receptors: pharmacological and clinical properties in the treatment of depression. *Pharmacological Reports*, *70*(1), 37–46. https://doi.org/10.1016/j.pharep.2017.07.011

Tang, S. W., & Tang, W. H. (2019). Opportunities in novel psychotropic drug design from natural compounds. *The International Journal of Neuropsychopharmacology*, *22*(9), 601–607. https://doi.org/10.1093/ijnp/pyz042

Umar, A. B., Uzairu, A., Shallangwa, G. A., & Uba, S. (2020). Docking - based strategy to design novel flavone - based arylamides as potent V600E - BRAF inhibitors with prediction of their drug - likeness and ADMET properties. *Bulletin of the National Research Centre*, *44*(1), 179. https://doi.org/10.1186/s42269-020-00432-7

Varadi, M., Anyango, S., Deshpande, M., Nair, S., Natassia, C., Yordanova, G., Yuan, D., Stroe, O., Wood, G., Laydon, A., Žídek, A., Green, T., Tunyasuvunakool, K., Petersen, S., Jumper, J., Clancy, E., Green, R., Vora, A., Lutfi, M., … Velankar, S. (2022). AlphaFold protein structure database: Massively expanding the structural coverage of protein-sequence space with high-accuracy models. *Nucleic Acids Research*, *50*(D1), D439–D444. https://doi.org/10.1093/nar/gkab1061

Waterhouse, A., Bertoni, M., Bienert, S., Studer, G., Tauriello, G., Gumienny, R., Heer, F. T., De Beer, T. A. P., Rempfer, C., Bordoli, L., Lepore, R., & Schwede, T. (2018). SWISS-MODEL: Homology modelling of protein structures and complexes. *Nucleic Acids Research*, *46*(W1), W296–W303. https://doi.org/10.1093/nar/gky427

Weichenberger, C. X., & Sippl, M. J. (2007). NQ-Flipper: Recognition and correction of erroneous asparagine and glutamine side-chain rotamers in protein structures. *Nucleic Acids Research*, *35*(Web Server), W403–406. https://doi.org/10.1093/nar/gkm263

Weichenberger, C. X., Byzia, P., & Sippl, M. J. (2008). Structural bioinformatics Visualization of unfavorable interactions in protein folds. *Bioinformatics (Oxford, England)*, *24*(9), 1206–1207. https://doi.org/10.1093/bioinformatics/btn108

Wiederstein, M., & Sippl, M. J. (2007). ProSA-web: interactive web service for the recognition of errors in three-dimensional structures of proteins. *Nucleic Acids Research*, *35*(Web Server), W407–410. https://doi.org/10.1093/nar/gkm290

Williams, C. J., Headd, J. J., Moriarty, N. W., Prisant, M. G., Videau, L. L., Deis, L. N., Verma, V., Keedy, D. A., Hintze, B. J., Chen, V. B., Jain, S., Lewis, S. M., Arendall, W. B., Snoeyink, J., Adams, P. D., Lovell, S. C., Richardson, J. S., & Richardson, D. C. (2018). MolProbity: More and better reference data for improved all-atom structure validation. *Protein Science: A Publication of the Protein Society*, *27*(1), 293–315. https://doi.org/10.1002/pro.3330

Wink, M. (2000). Interference of alkaloids with neuroreceptors and ion channels. *Studies in Natural Products Chemistry*, *21*, 3–122.

Wrońska, A. K., & Boguś, M. I. (2019). Harman and norharman, metabolites of the entomopathogenic fungus Conidiobolus coronatus (Entomophthorales), affect the serotonin levels and phagocytic activity of hemocytes, insect immunocompetent cells, in Galleria mellonella (Lepidoptera). *Cell & Bioscience*, *9*(1), 29–17. https://doi.org/10.1186/s13578-019-0291-1

Xu, P., Huang, S., Zhang, H., Mao, C., Zhou, X. E., Cheng, X., Simon, I. A., Shen, D. D., Yen, H. Y., Robinson, C. V., Harpsøe, K., Svensson, B., Guo, J., Jiang, H., Gloriam, D. E., Melcher, K., Jiang, Y., Zhang, Y., & Xu, H. E. (2021). Structural insights into the lipid and ligand regulation of serotonin receptors. *Nature*, *592*(7854), 469–473. https://doi.org/10.1038/s41586-021-03376-8

Yohn, C. N., Gergues, M. M., & Samuels, B. A. (2017). The role of 5-HT receptors in depression. *Molecular Brain*, *10*(1), 1–12. https://doi.org/10.1186/s13041-017-0306-y

Zrieq, R., Ahmad, I., Snoussi, M., Noumi, E., Iriti, M., Algahtani, F. D., Patel, H., Saeed, M., Tasleem, M., Sulaiman, S., Aouadi, K., & Kadri, A. (2021). Tomatidine and patchouli alcohol as inhibitors of SARS-CoV-2 enzymes (3CLpro, PLpro and NSP15) by molecular docking and molecular dynamics simulations. *International Journal of Molecular Sciences*, *22*(19), 10693–10622. https://doi.org/10.3390/ijms221910693